

## Ferromagnetism Induced by Clustered Co in Co-Doped Anatase TiO<sub>2</sub> Thin Films

J.-Y. Kim,<sup>1,2</sup> J.-H. Park,<sup>1,\*</sup> B.-G. Park,<sup>1</sup> H.-J. Noh,<sup>3</sup> S.-J. Oh,<sup>3</sup> J. S. Yang,<sup>4</sup> D.-H. Kim,<sup>4</sup> S. D. Bu,<sup>4</sup> T.-W. Noh,<sup>4</sup> H.-J. Lin,<sup>5</sup>  
H.-H. Hsieh,<sup>5</sup> and C. T. Chen<sup>5</sup>

<sup>1</sup>Department of Physics & Electron Spin Science Center, Pohang University of Science and Technology, Pohang, Korea

<sup>2</sup>Pohang Accelerator Laboratory, Pohang University of Science and Technology, Pohang, Korea

<sup>3</sup>School of Physics & Center for Strongly Correlated Materials Research, Seoul National University, Seoul, Korea

<sup>4</sup>School of Physics & Research Center for Oxide Electronics, Seoul National University, Seoul, Korea

<sup>5</sup>Synchrotron Radiation Research Center, Hsinchu 30077, Taiwan

(Received 14 April 2002; published 10 January 2003)

We investigated ferromagnetism of a newly discovered ferromagnetic semiconductor Co-doped anatase TiO<sub>2</sub> thin film, using the magnetic circular dichroism (MCD) at the Co  $L_{2,3}$  absorption edges. The magnetic moment was observed to be  $\sim 0.1 \mu_B/\text{Co}$  in the measurements, but the MCD spectral line shape is nearly identical to that of Co metal, showing that the ferromagnetism is induced by a small amount of clustered Co. With thermal treatments at  $\sim 400^\circ\text{C}$ , the MCD signal increases, and the moment reaches up to  $\sim 1.55 \mu_B/\text{Co}$ , which is  $\sim 90\%$  of the moment in Co metal. In the latter case, the cluster size was observed to be 20–60 nm.

DOI: 10.1103/PhysRevLett.90.017401

PACS numbers: 78.70.Dm, 68.37.Hk, 75.50.Pp, 87.64.Ni

There had been active studies on diluted magnetic semiconductors (DMS's), which were mostly composed of transition-metal magnetic impurities in II-VI semiconductors, for the last few decades [1]. The interests in DMS's surged again with a discovery of ferromagnetism in III-V based DMS such as Ga<sub>1-x</sub>Mn<sub>x</sub>As because of the possible technological applications utilizing both the semiconductor physics and the ferromagnetism, the so-called "spintronics" [2]. However, most of their Curie temperatures are much lower ( $T_C < 100$  K) than the room temperature so far. Meanwhile, oxide-based DMS's have buoyed up as candidates for room temperature DMS's. Indeed, Co-doped ZnO films were reported to show ferromagnetism with  $T_C \sim 300$  K. However, the reproducibility is somewhat questionable [3], and the origin of the ferromagnetism is uncertain.

Recently, cobalt doped anatase titanium dioxide, Ti<sub>1-x</sub>Co<sub>x</sub>O<sub>2</sub>, thin films were reported to be ferromagnetic even above 400 K [4] with a  $0.32 \mu_B/\text{Co}$  magnetic moment, and the magnetic ordering was explained in terms of the carrier-induced ferromagnetism [5] as in the III-V based DMS. The ferromagnetism of Ti<sub>1-x</sub>Co<sub>x</sub>O<sub>2</sub> was reproduced by Chambers *et al.* They reported that the moment is as high as  $1.25 \mu_B/\text{Co}$ , and claimed that the ferromagnetism strongly depends on the oxygen deficiency [6,7]. These results seem to show that the ferromagnetism in Ti<sub>1-x</sub>Co<sub>x</sub>O<sub>2</sub> is originated from the ordered low spin Co<sup>2+</sup> state due to the charge carriers induced by oxygen defects. However, considering the fact that the ferromagnetism strongly depends on the growth condition [7], the possibility of the Co segregation cannot be excluded in this system [8]. Furthermore, it was reported that the anatase TiO<sub>2</sub> is a crystalline defected easily [9]. Therefore it is important to clarify the origin of ferromagnetism in the oxide-based high  $T_C$  DMS.

In this Letter, we report the x-ray absorption spectroscopy (XAS) and magnetic circular dichroism (MCD) results at the Co  $L_{2,3}$  edges to clarify the ferromagnetic origin of Co-doped anatase TiO<sub>2</sub> thin films. The XAS has been well known to be a very useful probe to determine the electronic and magnetic states [10], and its MCD signal reflects only the ferromagnetic origin [11]. In the study, we found that in the epitaxially grown Ti<sub>1-x</sub>Co<sub>x</sub>O<sub>2</sub> films, the Co state is a divalent high spin ionic state, Co<sup>2+</sup> ( $3d^7$ ;  $S = 3/2$ ), as in CoO, indicating that the doped Co ions could be well substituted for the Ti sites. However, we observed a small MCD signal at the Co  $L_{2,3}$  edges, which corresponds to  $\sim 0.1 \mu_B/\text{Co}$ , and the MCD line shape is nearly identical to that of Co metal, suggesting that the magnetic origin should be a small amount of clustered Co. Furthermore, after thermal treatments at  $\sim 400^\circ\text{C}$ , the MCD signal becomes greatly enhanced, and the moment reaches up to  $\sim 1.55 \mu_B/\text{Co}$ , which is about 90% of the moment in Co metal. The MCD line shape does not change under the thermal treatment, while the XAS line shape gradually changes and becomes finally similar to that of Co metal. The field-emitted scanning electron microscope (FE-SEM) image of the postannealed sample shows that Co clusters were formed randomly in the entire sample with 20–60 nm in size. These results manifest that the ferromagnetism in the Co-doped anatase TiO<sub>2</sub> is induced by the Co clustering.

The 40 nm thick anatase Ti<sub>1-x</sub>Co<sub>x</sub>O<sub>2</sub> films with different  $x$  values were grown on LaAlO<sub>3</sub> (001) substrates with laser molecular beam epitaxy [12,13]. Each Ti<sub>1-x</sub>Co<sub>x</sub>O<sub>2</sub> ceramic target was ablated by a KrF pulsed laser with  $2 \text{ W}/\text{cm}^2$ . The substrate temperature and the O<sub>2</sub> partial pressure during the growth were maintained at  $650^\circ\text{C}$  and  $10^{-5}$  to  $10^{-6}$  Torr, respectively. The growth rates were less than  $1 \text{ \AA}/\text{min}$ . The growing surfaces were

monitored *in situ* with the reflection high energy electron diffraction (RHEED). The structural properties of the films were confirmed by *in situ* RHEED and *ex situ* x-ray diffraction (XRD).

Figure 1 shows the RHEED intensity oscillations of the specular spot during the growth of a  $\text{Ti}_{0.93}\text{Co}_{0.07}\text{O}_2$  film. After deposition of about one unit cell, which corresponds to 4  $\text{TiO}_2$  monolayers, a clear oscillation became observable, indicating that the film was grown epitaxially in the layer-by-layer growth mode. The clear and streaky RHEED pattern in the inset confirms that the film is in the anatase phase with a very flat surface. As shown in the intensity line profile presented in the figure, three weak streaks, which are due to the intrinsic  $(4 \times 1)$  surface reconstruction, appear between the specular streak in the center and the 1st order diffraction streak [14], and provide other evidence for the formation of the anatase phase. Furthermore, XRD of the film shows only sharp  $(00l)$  peaks of the anatase phase. Systematic study for the sample growth by using the transmitted electron microscopy (TEM) also confirms that the layer-by-layer growth provides the high quality epitaxial films without any detectable phase segregation [12].

The XAS and x-ray magnetic circular dichroism (XMCD) measurements were carried out at the Dragon beamline at the Synchrotron Radiation Research Center in Taiwan. The energy resolutions of incident light were set to be 0.3 and 0.5 eV and the polarization of the light was chosen to linear and circular for the XAS and XMCD measurements, respectively. The XAS and XMCD spectra were obtained in a total electron yield mode with an  $\sim 100$  Å probing depth. The samples were introduced in an UHV experimental chamber [15]. The pressure during the measurements was below  $1 \times 10^{-9}$  Torr, and the sample temperature was maintained at 300 K.

In order to check the Co state, we performed Co  $L_{2,3}$ -edge XAS measurements on  $\text{Ti}_{1-x}\text{Co}_x\text{O}_2$  ( $x = 0.04, 0.07, 0.10$ ) thin films. The spectra are presented in Fig. 2, in comparison with the reference spectrum of CoO. The

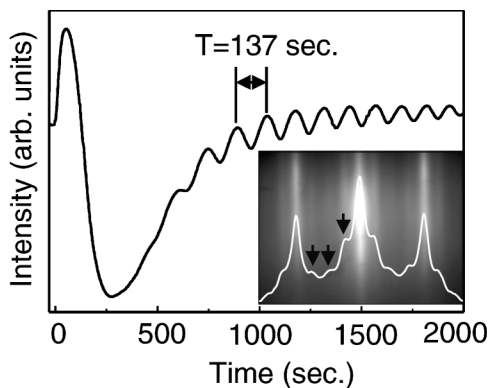


FIG. 1. RHEED oscillations during the deposition. The inset shows the RHEED pattern and corresponding intensity-line profile. Three additional lines marked by three arrows represent a weak  $(4 \times 1)$  surface reconstruction pattern.

spectra, which result from the Co  $2p \rightarrow 3d$  dipole transitions, are dominated by the large  $2p$  core-hole spin-orbit coupling energy dividing the spectra into roughly the  $L_3$  and  $L_2$  regions at low and high photon energies, respectively. As shown in the figure, the spectra are nearly identical for different  $x$  values, and display a characteristic multiplet structure. In comparison with the spectrum of CoO, one can recognize that the spectra of  $\text{Ti}_{1-x}\text{Co}_x\text{O}_2$  are very similar to that of CoO. The absorption white line locates at exactly the same energy and the overall multiplet structure is very similar except for minor differences in the relative intensities of the multiplet states at the  $L_3$  edge, which are probably due to a small tetragonal distortion of the  $\text{CoO}_6$  octahedron in the anatase structure. The whiteline energy and the multiplet structure represent the valence and the ionic ground state symmetry, respectively. Therefore, we can confidently conclude that the ionic ground state of doped Co in  $\text{Ti}_{1-x}\text{Co}_x\text{O}_2$  is the high spin divalent state, i.e.,  $\text{Co}^{2+}$  ( $3d^7$ ;  $S = 3/2$ ), as in CoO. For further confirmation, theoretical multiplet model calculations were carried out for the XAS spectra for a high spin  $\text{Co}^{2+}$  ( $S = 3/2$ ) and a low spin  $\text{Co}^{2+}$  ( $S = 1/2$ ) ground state under  $O_h$  symmetry [16]. As shown in the figure, the spectra of  $\text{Ti}_{1-x}\text{Co}_x\text{O}_2$  and CoO are generally well reproduced by the calculation for the high spin  $\text{Co}^{2+}$ . These results show that the Co state in  $\text{Ti}_{1-x}\text{Co}_x\text{O}_2$  is a Co-oxide state with the high spin  $\text{Co}^{2+}$  as in CoO, different from the previous interpretation of the low spin  $\text{Co}^{2+}$  [6].

Figure 3 shows the XAS and XMCD spectra at the Co  $L_{2,3}$  edges of  $\text{Ti}_{0.90}\text{Co}_{0.10}\text{O}_2$  for different annealing times. The samples were *in situ* annealed at  $\sim 400$  °C under  $10^{-6}$  Torr  $\text{O}_2$ , which is relatively lower than the growth temperature (i.e., 650 °C). For the XMCD measurements, the degree of circular polarization of the incident light was set to be 0.85, and a 0.6 T magnetic field produced by

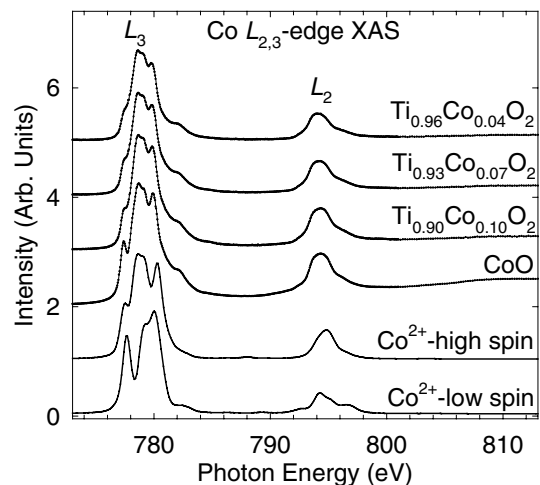


FIG. 2. Co  $L_{2,3}$ -edge XAS spectra of  $\text{Ti}_{1-x}\text{Co}_x\text{O}_2$  ( $x = 0.04, 0.07, 0.10$ ) in comparison with those of CoO and theoretical calculation spectra for high spin  $\text{Co}^{2+}$  ( $3d^7$ ;  $S = 3/2$ ) and low spin  $\text{Co}^{2+}$  ( $3d^7$ ;  $S = 1/2$ ) states under  $O_h$  symmetry.

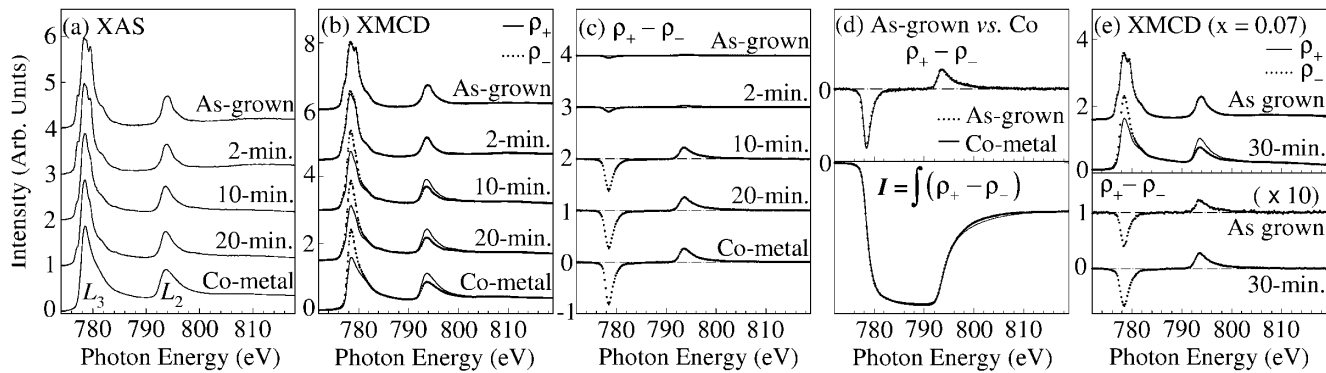


FIG. 3. XMCD spectra of  $\text{Ti}_{1-x}\text{Co}_x\text{O}_2$  for the different postannealing times  $T_A = 0$  (as grown), 2, 10, and 20 min in comparison with those of Co metal. (a) Co  $L_{2,3}$ -edge XAS spectra of the  $x = 0.10$ , (b) Co  $L_{2,3}$ -edge XMCD spectra of the  $x = 0.10$ , (c) MCD signal;  $\rho_+ - \rho_-$  of the  $x = 0.10$ , (d) comparison of MCD signals and their integrations for the as-grown  $x = 0.10$  sample and Co metal, and (e) XMCD results of the  $x = 0.07$  sample.

an electromagnet was applied along the surface normal of the sample to align the spin moment. In order to minimize the artificial effects caused by a decrease of the photon flux with time, the spin direction was flipped to be parallel ( $\rho_+$ ) and antiparallel ( $\rho_-$ ) to the photon helicity vector at each data point. The spectra for the different spin directions ( $\rho_+$  and  $\rho_-$ ), which were normalized by the photon flux, and the dichroism spectra ( $\rho_+ - \rho_-$ ) are presented in the figure, where the degree of circular polarization was taken into account.

One can recognize that the ionic multiplet structure of the Co  $L$ -edge XAS spectrum is continuously smeared out with an increase of the annealing time,  $T_A$ . After 20-min annealing, the spectral line shape rather resembles that of Co metal. As shown in Fig. 3(c), the weak MCD signal observed in the as-grown film greatly increases with the annealing time, without any significant change in the line shape. In comparison of the MCD spectrum ( $\rho_+ - \rho_-$ ) and its integration ( $I$ ) of the as-grown  $\text{Ti}_{0.90}\text{Co}_{0.10}\text{O}_2$  with those of Co metal, Fig. 3(d) shows nearly identical line shapes for both, showing that the magnetic origin of  $\text{Ti}_{0.90}\text{Co}_{0.10}\text{O}_2$  is the same as Co metal. According to the sum rule [17], the similar line shape of the integration means about the same spin-to-orbital moment ratio. The intensity of the magnetic signal is estimated to be about 6% ( $\sim 0.1\mu_B/\text{Co}$ ), 11% ( $\sim 0.2\mu_B/\text{Co}$ ), 75% ( $\sim 1.3\mu_B/\text{Co}$ ), and 90% ( $\sim 1.55\mu_B/\text{Co}$ ) of that of Co metal ( $1.72\mu_B/\text{Co}$ ) for  $T_A = 0, 2, 10,$  and 20 min, respectively. These results clearly show that the ferromagnetism in the Co-doped anatase  $\text{TiO}_2$  is originated from clustered Co metal, rather than the ionic oxide Co, and the amount of clustered Co metal in an as-grown sample increases greatly with the postannealing. Such behaviors were also observed in the 4% and 7% Co-doped samples as shown for the  $x = 0.07$  sample in Fig. 3(e). Hence, the amount of clustered Co is expected to depend on the growth condition, and the observed large variation of the ordered moment is somehow natural in this system [12]. In general, the Co-metal surface is easily oxidized even in a low  $\text{O}_2$  partial pressure (below  $10^{-6}$  Torr), and thus the Co

clustering is somewhat striking in the oxide-based material. However, the anatase  $\text{TiO}_2$ , which is a well-known catalyst, yields defects so easily [9], and it seems to offer a room for the Co clustering.

The postannealing turns out to accelerate greatly the Co clustering in Co doped anatase  $\text{TiO}_2$  systems, and the ordered moment reaches up to  $\sim 1.55\mu_B/\text{Co}$ , indicating that the Co clusters become considerably large. Figure 4 shows the *ex situ* FE-SEM pictures of the  $\text{Ti}_{1-x}\text{Co}_x\text{O}_2$  ( $x = 0.00, 0.10$ ) after the 20-min postannealing. The picture of the  $x = 0.00$  sample shows just dark background due to the insulating character, while that of the  $x = 0.10$  sample clearly shows small islands of the clustered Co, which are almost randomly distributed in the entire range. The metallic character of Co makes the image quite visible. The size of the Co island ranges from 20 to 60 nm.

Although the postannealing was performed at relatively low temperature, the annealing possibly redistributes the amount of Co. However, a wide energy range XAS measurement shows that there is no considerable variation in the amount of Co in the range of the XAS probing depth ( $\sim 100$  Å) [18]. The Ti  $L$ -edge and O  $K$ -edge spectra do not show any change in the line shape before and after the postannealing, indicating that there is no hint of structural transition to the rutile  $\text{TiO}_2$ , which shows quite different XAS spectral line shape at both edges [19]. However, the higher temperature annealing

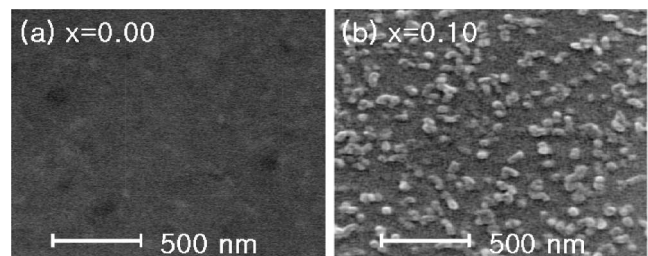


FIG. 4. FE-SEM images of anatase (a)  $\text{TiO}_2$  and (b)  $\text{Ti}_{0.90}\text{Co}_{0.10}\text{O}_2$  after the postannealing.

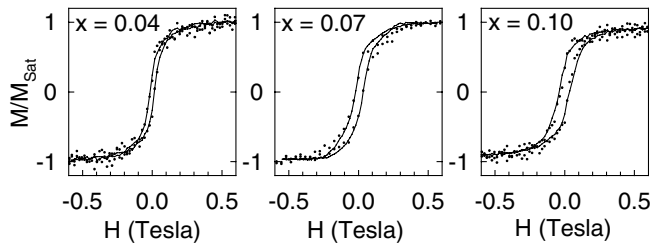


FIG. 5. In-plane (dotted lines) and along the surface normal (solid lines) magnetic hysteresis curves of anatase  $\text{Ti}_{1-x}\text{Co}_x\text{O}_2$  ( $x = 0.04, 0.07, 0.10$ ) after the postannealing.

(30-min at  $\sim 650^\circ\text{C}$ ) was found to increase considerably the Co intensity relative to those of Ti and O [18], indicating the movement of Co into the surface region.

Figure 5 shows the magnetic hysteresis ( $M$  vs  $H$ ) curves, which were obtained from the XMCD intensity at the Co  $L_3$  white line, of the postannealed  $\text{Ti}_{1-x}\text{Co}_x\text{O}_2$  ( $x = 0.04, 0.07, 0.10$ ) films at  $\sim 400^\circ\text{C}$ . For all three samples, there is not much difference in the  $M$  vs  $H$  for the applied magnetic field in the plane and along the surface normal, indicating no considerable magnetic anisotropy [20]. However, the magnetic coercivity increases with the amount of Co. The coercive fields are estimated to be about 150, 250, and 400 Oe for  $x = 0.04, 0.07$ , and 0.10, respectively. At this moment, we are not sure whether the coercive field results from that of each island or from the magnetic correlation between islands.

The Curie temperature of the system is expected to be similar to that of Co metal ( $T_C = 1388\text{ K}$ ). However, the  $M$  vs  $T$  measurement of the Co-doped  $\text{TiO}_2$  is somewhat meaningless. Under low  $\text{O}_2$  partial pressure (below  $10^{-6}$  Torr), the Co clustering proceeds above  $\sim 400^\circ\text{C}$ , while under high  $\text{O}_2$  partial pressure as in air, we found that the ferromagnetism completely disappeared above  $\sim 400^\circ\text{C}$  due to oxidization of the clustered Co.

In conclusion, we investigated the origin of ferromagnetism observed in Co-doped anatase  $\text{TiO}_2$  films using the x-ray magnetic circular dichroism at the Co  $L_{2,3}$  edges. The substituted Co has a high spin  $\text{Co}^{2+}$  as in CoO, but the magnetic signal, which contributes to  $\sim 0.1\mu_B/\text{Co}$  in average, was found to be identical to that of Co metal, showing that the magnetic origin is a partial amount of clustered Co. The magnetic signal was enhanced greatly with thermal treatments, and the magnetic moment reached up to  $\sim 1.55\mu_B/\text{Co}$ , which corresponds to about 90% of the moment in Co metal, indicating that most of Co becomes clustered during the postannealing process. The Co clusters, which are 20 to 60 nm in size, are distributed randomly in the entire surface region.

This work was supported by a Korea Research Foundation grant (KRF-2000-15-DS0015). J.-Y. Kim acknowledges the financial support through the Future Basic Technology project by MOST, Korea. The work was also supported by KOSEF through eSSC at POSTECH and CSCMR at SNU, Ministry of Science and Tech-

nology through the Created Research Initiative program, POSTECH basic research fund, and BK21 project of Ministry of Education, Korea.

\*Author to whom all correspondence should be addressed.  
Email address: jhp@postech.ac.kr

- [1] *Diluted Magnetic Semiconductors, Semiconductors and Semimetals*, edited by J.K. Furdyna and J. Kossut (Academic, New York, 1988), Vol. 25; *Diluted Magnetic Semiconductors*, edited by M. Jain (World Scientific, Singapore, 1991).
- [2] R. Fiederling *et al.*, Nature (London) **402**, 787 (1999); Y. Ohno *et al.*, *ibid.* **402**, 790 (1999); T. Dietl *et al.*, Science **287**, 1019 (2000).
- [3] K. Ueda, H. Tabata, and T. Kawai, Appl. Phys. Lett. **79**, 988 (2001).
- [4] Y. Matsumoto *et al.*, Science **291**, 854 (2001).
- [5] J. König, H.-H. Lin, and A. H. MacDonald, Phys. Rev. Lett. **84**, 5628 (2000).
- [6] S. A. Chamber *et al.*, Appl. Phys. Lett. **79**, 3467 (2001).
- [7] S. A. Chamber, Materialstoday April, 34 (2002).
- [8] S. R. Shinde *et al.*, cond-mat/0203576.
- [9] G. S. Herman, M. R. Sievers, and Y. Gao, Phys. Rev. Lett. **84**, 3354 (2000); T. Uustare, J. Aarik, and M. Elango, Appl. Phys. Lett. **65**, 2551 (1994).
- [10] F. M. F. de Groot *et al.*, Phys. Rev. B **42**, 5459 (1990).
- [11] C. T. Chen *et al.*, Phys. Rev. Lett. **75**, 152 (1995); J.-H. Park *et al.*, Phys. Rev. Lett. **81**, 1953 (1998); G. Schutz *et al.*, Phys. Rev. Lett. **58**, 737 (1987).
- [12] D. H. Kim *et al.*, Appl. Phys. Lett. **81**, 2421 (2002). The TEM image shows no hint of phase segregation in the sample grown in the layer-by-layer mode, while Co clusters become observable in the sample grown in the island growth mode under lower  $\text{O}_2$  pressure.
- [13] B. H. Park *et al.*, Appl. Phys. Lett. **79**, 2797 (2001).
- [14] Y. Liang, S. Gan, S. A. Chambers, and E. I. Altman, Phys. Rev. B **63**, 235402 (2001).
- [15] The core-level photoemission shows that the surface contamination is mostly due to chemisorbed  $\text{CO}_2^-$  molecules, which do not affect the XMCD results.
- [16] Refer to K. Cho *et al.*, Phys. Rev. B **63**, 155203 (2001), for the details of the calculation method. The  $\text{O}_h$  crystal field splitting energy  $10Dq = 0.6\text{ eV}$  for the high spin state ( $S = 3/2$ ) and  $10Dq = 2\text{ eV}$  for the low spin state ( $S = 1/2$ ). The other parameters are the on-site Coulomb  $U = 5\text{ eV}$ , the charge transfer energy  $\Delta = 6\text{ eV}$ , and the  $p-d$  hybridization energy  $V_{pd\sigma} = 1.5\text{ eV}$  for both states.
- [17] B. T. Thole, P. Carra, F. Sette, and G. van der Laan, Phys. Rev. Lett. **68**, 1943 (1992); P. Carra, B. T. Thole, M. Altarelli, and X. Wang, *ibid.* **70**, 694 (1993).
- [18] J.-H. Park *et al.* (to be published).
- [19] G. van der Laan, Phys. Rev. B **41**, 12366 (1990).
- [20] The in-plane and along the surface normal hysteresis curves were obtained from fluorescence and total electron yields, which have probing depths of  $\sim 1000\text{ \AA}$  and  $\sim 100\text{ \AA}$ , respectively. But this difference seems not to affect the magnetic hysteresis as confirmed in the magneto-optic Kerr effect measurements.